Research Article

Chemical Review and Letters
journal homepage: www.chemrevlett.com
ISSN (online): 2645-4947 (print) 2676-7279

Enhancing energy efficiency of LPG separation units through pinch-based heat integration in refinery operations

Ahmed Ould Brahim[1,2,] *, Souad Abderafi[1,2]

[1]*LASPI, Mohammadia Engineering School, Mohammed V University in Rabat, Ibn Sina, B.P. 765, Agdal, Rabat, 10090, Morocco.*
[2]*SMC, Nouakchott University, B.P. 5026. Nouakchott, Mauritania.*

ARTICLE INFO

Article history:
Received 15 September 2025
Received in revised form 13 December 2025
Accepted 14 December 2025

Keywords:
Energy efficiency
Energetic integration
Debutanizer column
Splitter column
LPG separation

ABSTRACT

The separation of Liquefied Petroleum Gas (LPG) in oil refineries typically relies on two highly energy-intensive distillation columns: the debutanizer and the splitter. Their significant heat demand contributes directly to elevated operating costs and greenhouse gas emissions. This study aims to enhance the energy efficiency of these units through a heat-integration strategy based on Pinch Technology. Industrial operating data from an active refinery were used to simulate the existing configuration in PRO/II software employing the Peng–Robinson equation of state. The model was validated, showing satisfactory agreement between simulated and actual plant performance. A new heat-integrated configuration was then proposed by introducing three process-to-process heat exchangers to recover and reuse thermal energy within the LPG separation train. Simulation of the optimized design reveals a 23.46% reduction in overall energy consumption and a 33.17% decrease in CO_2 emissions compared with the conventional setup. These results demonstrate that systematic heat integration offers an effective pathway to improving both the energy and environmental performance of LPG distillation systems.

1. Introduction

Crude oil refining produces various petroleum products, including diesel, jet fuel, and petroleum gases [1]. The latter are liquefied to form Liquefied Petroleum Gas (LPG), which burns cleaner than gasoline and diesel [1,2]. LPG is widely used as a fuel for vehicles such as cars and motorcycles, and as a secondary energy source in residential heating [3]. It is also recognized for its superior energy efficiency compared to other petroleum derivatives and is suitable for use as a refrigerant, helping to mitigate ozone layer depletion [4].

LPG is primarily composed of two non-toxic, flammable gases: propane (C_3H_8) and butane (C_4H_{10}) [4,5]. Its composition varies seasonally—propane predominates in winter, while butane is more prevalent in summer [5,6]. The separation of these components is achieved by heating crude oil to elevated temperatures and feeding it into a series of distillation columns to isolate the desired products.

Several recent studies, including those by Suphanit [7] and Kiss et al. [8], have proposed advanced distillation technologies aimed at improving energy efficiency. However, these studies lack detailed techno-economic evaluations of the proposed column configurations. The selection of an optimal distillation technology depends on various operational parameters and specific process requirements. Retrofitting a refinery to implement more efficient technologies typically involves substantial capital investment, as demonstrated by a case study based on real data from a Nigerian refinery, which revealed significant inefficiencies in its existing processes [9].

Conventional distillation remains the most commonly used method for separation in industrial chemical processing, but it is highly energy-intensive. Previous studies have estimated that distillation processes can account for more than 70% of a refinery's total energy consumption [12]. Consequently, crude oil refining is among the most polluting industrial sectors, due to the substantial greenhouse gas emissions associated with high energy usage, which also drives up operational costs [13,14].

* Corresponding author E-mail: ahmed.ouldbrahim0101@gmail.com
https://doi.org/10.22034/crl.2025.529567.1695

Significant international research has therefore focused on optimizing energy use in distillation columns, particularly for the separation of petroleum products [15–25]. Funmilayo et al. [15] proposed a strategy based on artificial neural networks (ANN) to enhance the generalization of exergy efficiency models using operational data. Their approach maximized energy performance while maintaining product quality and throughput.

Al-Mayyahi et al. [16] employed a multi-objective optimization method (genetic algorithm, NSGA-II) to study the impact of crude pre-flash on energy consumption and CO_2 emissions in atmospheric distillation units (CDU). Their results indicated that crude pre-flash significantly reduces CO_2 emissions at high residue yields but offers limited benefits at low yields.

Wahid et al. [17] developed a reconfiguration strategy for crude oil distillation units, segmenting the system into sub-units including the prefractionator unit (PFU), atmospheric distillation unit (ADU), vacuum distillation unit (VDU), separation unit (SPU), stabilization unit (SBU), and a heat exchanger network (HEN). Applied to a Nigerian refinery, their retrofit design achieved notable energy savings and proved both economically viable and environmentally beneficial. Liu et al. [25] explored a novel design for the absorption stabilization unit aimed at improving refinery energy efficiency. Their configuration achieved reductions in hot and cold utility demands of 17.98% and 25.65%, respectively, with a favorable payback period. Other studies have focused on the sensitivity of operational parameters for optimization. Brahmani et al. [19] investigated parametric sensitivity in LPG and natural gas liquids (NGL) stabilization columns to identify optimal conditions that enhanced LPG production and reduced CO_2 emissions in an Iranian gas refinery. Similarly, Ould Brahim et al. [7] analyzed the effect of operational parameters on energy efficiency in gasoline stabilization columns, aiming for improved energy use and lower costs. Techniques such as response surface methodology, ANN, and genetic algorithms have also been applied in this context [20–22]. This literature review highlights several optimization methods used to minimize energy consumption in distillation units. These include artificial intelligence techniques (e.g., ANN, genetic algorithms), design modification through heat integration, and sensitivity analysis to determine optimal operating parameters. While many of these methods have been applied to atmospheric distillation, demethanization, gas dehydration, and absorption-stabilization units, few studies have targeted LPG-specific distillation columns. One notable exception is the work of Díez et al. [23], who simulated a heat pump-integrated i-butane/n-butane separation process and evaluated its performance under new configurations. Building on this state-of-the-art review, the present study focuses on optimizing the energy performance of two key units in the LPG separation process: the debutanizer and splitter columns. The primary objective is to improve energy efficiency and reduce CO_2 emissions in an existing refinery. This is achieved by proposing a new heat-integrated column configuration and evaluating its performance using simulation tools (PRO/II) to analyze column stream characteristics.

2. Materials and Methods

2.1. Process description and industrial data

The petroleum refining process is complex, comprising multiple separation units that yield a spectrum of hydrocarbon fractions, along with trace amounts of sulfur, oxygen, nitrogen, and metals. Crude feed is first heated to approximately 400 °C and introduced into an atmospheric distillation column, where components are separated by volatility: light products such as butane rise to the column top, while heavier cuts—gasoline, kerosene, and gas oil—are drawn off at successively lower trays [5]. Non-volatile residues remain at the column bottom.

This study focuses on the LPG separation section, which isolates propane and butane from lighter naphtha fractions. As shown in Figure 1, two sequential distillation columns perform this task. The first column, the debutanizer, contains 29 theoretical stages and is fed at stage 11 with a vapor–liquid mixture at 548.89 kmol/h, 101 °C, and 11.7 bar. Overhead vapor is condensed by cooling water to yield the LPG product, while the stabilized C_5^+ gasoline remains at the bottom.

The condensed LPG stream (117.27 kmol/h, 44 °C, 18.66 bar) then feeds the second column—the splitter—at stage 12. This 32-stage column fractionates the LPG into butane (bottom product) and propane (overhead product). The propane-rich vapor is subsequently cooled in an air-cooled heat exchanger. Both columns receive their feeds from the Merox sweetening unit and a reformate circuit; although both streams enter at 11 bar and 101 °C, they differ in composition and flow rate. Industrial operating data are summarized in Table 1.

Light naphtha cuts often contain trace mercaptans that impart unpleasant odors. These are removed in the Merox unit, which also increases the gasoline's octane number.

2.1.1. Distillation column modeling

Distillation is a separation technique that exploits differences in component volatility within a liquid mixture. A typical distillation column consists of a series of trays, numbered from top to bottom, where counter-current vapor–liquid mass transfer occurs. Heat $Q_r$is supplied at the column base through a reboiler to vaporize part of the liquid and drive the separation, while heat $Q_c$is removed at the top via a condenser to liquefy the overhead vapor.

Table 1. Industrial data for the LPG recovery and splitter process

	LPG recovery	LPG Splitter
Trays number	29	32
Feed tray position	11	12
Refux ratio	1.4	2
Feed flow rate F (k.mol/h)	548.89	117.27
Feed temperature (°C)	101	44
Feed pressure P (bar)	11.7	18.66
P_{Head}(bar)	7.6	17
P_{Botom}(bar)	8.8	18
Temp Top (°C)	52.65	66.73
Temp Bott (°C)	142	97.80

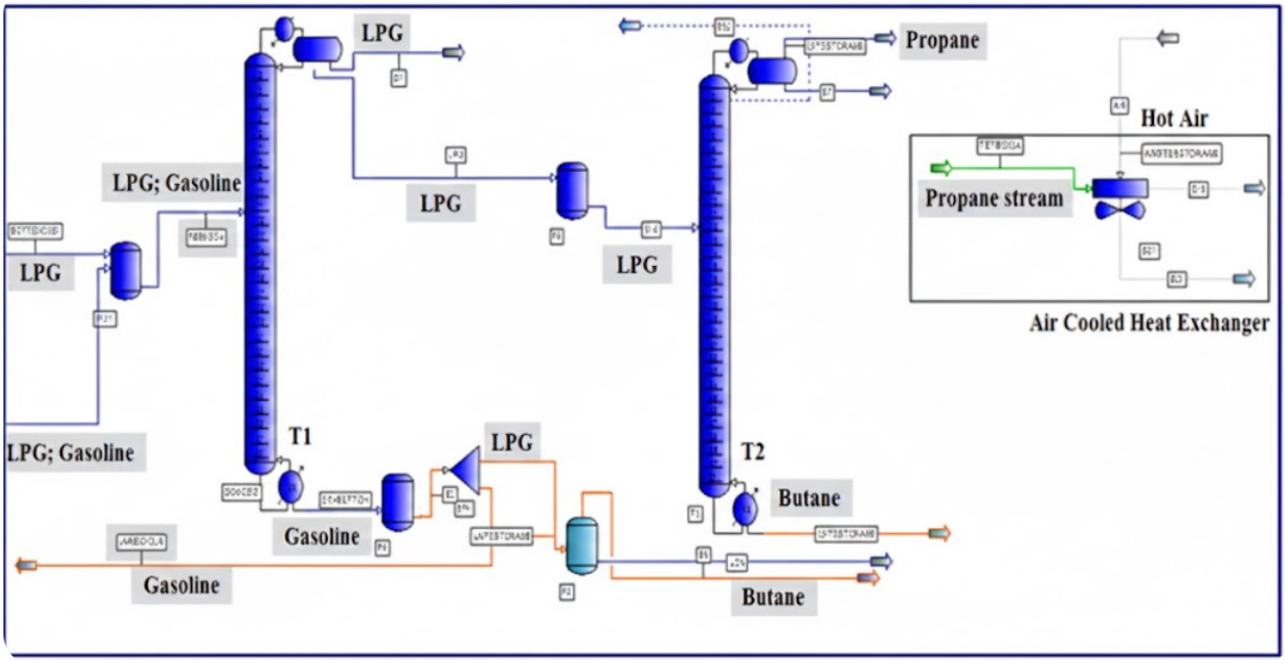

Fig. 1. Simplified schematic of the LPG separation process

Figure 2 presents a schematic representation of a conventional distillation column. The feed stream characterized by its flow rate F, mass-fraction composition z_f, pressure P, and temperature $T$is introduced at a designated tray, dividing the column into a rectifying section above the feed and a stripping section below it. The more volatile components preferentially migrate upward and are withdrawn at the top, whereas the less volatile components flow downward. The overhead vapor is condensed, and a portion of the condensate is returned as reflux to enhance separation efficiency, while the remainder is withdrawn as the distillate product [28].

The following section presents the mathematical model used to simulate the LPG separation system, which consists of two interconnected distillation columns. Each column is described using component mass balances, energy balances, and vapor–liquid equilibrium (VLE) relations.

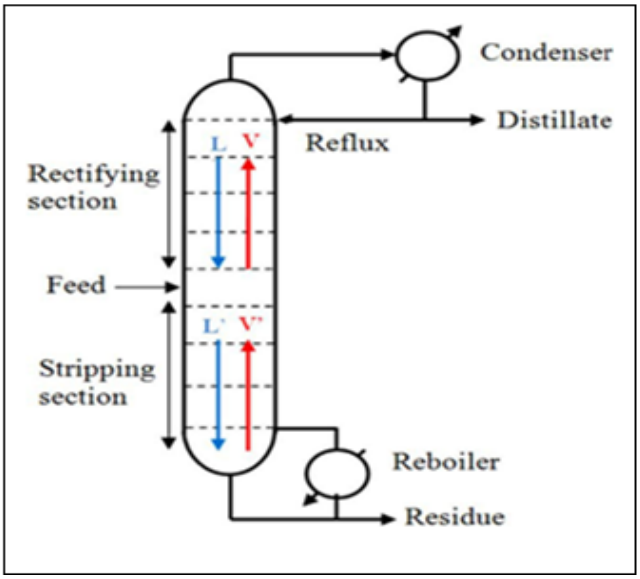

Fig. 2 Schematic representing distillation column

2.1.2. Material and Energy balances

The steady-state modeling of a distillation column relies on several standard assumptions. All trays are considered to be in vapor–liquid equilibrium, the pressure is uniform throughout the column, and the system operates adiabatically, with no heat exchange with the surroundings.

Total condensation is assumed at the condenser, and variations in composition and molar enthalpy across the feed stage are neglected. Under these conditions, component material and energy balances can be established for each stage [28].

Figure 3 illustrates a generic equilibrium stage. At stage j, the system may receive a feed stream F_j, a descending liquid flow L_{j-1}, and an ascending vapor flow V_{j+1}. Depending on the column configuration, additional streams such as a side liquid withdrawal U_j, a side vapor withdrawal W_j, or a heat input $Q_j$may also be present.

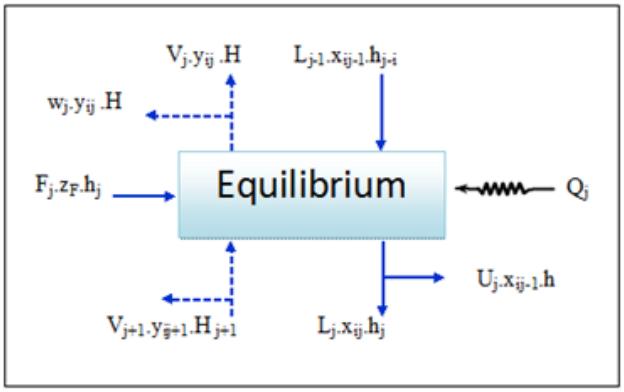

Fig. 3. Principle of an equilibrium tray

The equations of balance material and energy that govern the operation of the column are given bellow:

- Material balance equation for each component i:

$$L_{j-1}x_{ij-1} - (V_j + W_j)y_{ij} - (L_j + U_j)x_{ij} + V_{j+1}y_{ij+1}F_jz_{ij} = 0 \quad (1)$$

- Energy balance equation

$$L_{j-1}h_{j-1} - (V_j + W_j)H_{ij} - (L_j + U_j)h_j + V_{j+1}h_{ij+1}F_jh_{Fj} - Q_j = 0 \quad (2)$$

Where, V and L are vapor and liquid flow rate, respectively (in kg/h); U and w liquid and vapor side stream flow, respectively (in kg/h). The liquid and vapor composition is expressed in mass fractions.

The heat quantities in the boiler and in the condenser are calculated from the following equations:

$$Q_1 = V_2h_2 - (U_1 + L_1)h_1 - V_1h_1 \quad (3)$$

$$Q_n = V_nh_n + U_nh_n - L_{n-1}h_{n-1} \quad (4)$$

Where, Q_1 is heat flow of condenser and Q_n is heat flow of reboiler

2.1.3. VLE calculation

The calculation of Vapor–Liquid Equilibrium (VLE) is based on the principle that, at equilibrium, the fugacity of each component in the liquid phase is equal to that in the vapor phase at the same temperature and pressure [29]:

$$f_i^L = f_i^V \quad (5)$$

Where, $\boldsymbol{f_i^L}$ and $\boldsymbol{f_i^V}$ are fugacities of component i in liquid and vapor phase, respectively, at the same temperature and pressure, expressed by:

$$f_i^L = x_i\phi_i^L P \quad (6)$$

$$f_i^V = y_i\phi_i^V P \quad (7)$$

The calculation of the fugacity coefficient φi. in both the liquid and vapor phases requires a thermodynamic model, typically an equation of state (EOS). Among the available cubic EOS of the Van der Waals type, the Soave–Redlich–Kwong (SRK) and Peng–Robinson (PR) models are the most widely used due to their simplicity and flexibility, particularly for hydrocarbon systems [17, 25, 26]. The PR EOS, in particular, has proven to be more reliable for predicting the vapor–liquid equilibria (VLE) of light hydrocarbons, especially at high pressures [26]. Furthermore, a comparison of simulation results for heat duties and stream properties has shown that the PR model yields smaller errors than the SRK model.PR model has the following form for a pure component [30]:

$$P = \frac{RT}{v-b} - \frac{a(T)}{v(v+b)+b(v-b)} \quad (8)$$

Where P is the absolute pressure, T is the absolute temperature, V is the molar volume, and R is the universal gas constant.

The volume and energy parameters a and b of the Peng–Robinson Equation of State (PR EOS) are calculated using the following correlations:

$$a(T) = a_c\alpha(\omega, T_r) \quad (9)$$

$$a_c = 0.4572\frac{R^2T_c^2}{P_c} \quad (10)$$

$$\sqrt{\alpha} = 1 + m\left(1 - \sqrt{\frac{T}{T_c}}\right) \quad (11)$$

$$b = 0.07780\frac{RT_c}{P_c} \quad (12)$$

Where, subscripts, c and r denote critical and reduced conditions, respectively; m depends on the acentric factor, ω:

$$m = 0.37464 + 1.54226\omega - 0.26992\omega^2 \quad (13)$$

To extend the Peng–Robinson Equation of State (PR EOS) to mixtures, it is necessary to account for the composition of the system. Several algebraic mixing rules have been proposed for this purpose. In this work, we adopt the classical Van der Waals one-fluid mixing

rules, as recommended for use with the PR EOS [31]. These rules are used to calculate the mixture parameters a_m and b_m from the pure-component parameters as follows:

$$a_m = \sum_i \sum_j x_i\, x_j \left(a_i a_j\right)^{0.5}\left(1 - k_{ij}\right) \quad (14)$$

$$b_m = \sum_i x_i\, bi \quad (15)$$

k_{ij}, is the binary interaction parameter between component i and j; with $k_{ij}=k_{ji}$ and $k_{ii}=0$.

2.2. Optimization methodology

In this study, an energy integration method known as Pinch Technology is employed to reduce energy consumption and greenhouse gas emissions. This method aims to enhance energy efficiency by establishing thermodynamically optimal heat exchange between hot and cold process streams. By applying thermodynamic principles, it becomes possible to better allocate heat exchanger surface areas across the system, thereby maximising energy recovery and minimising the external utility requirements. In the following section, we present the methodology used to reduce energy consumption, describe the models applied for heat exchanger design, and explain how the overall performance of the studied process was evaluated.

2.2.1. Pinch technology procedure

In conventional distillation processes, heat is supplied to the feed heater and the reboiler to achieve separation of the components. However, a significant portion of this heat is subsequently rejected in the condenser, which cools the overhead vapour stream [8]. Through heat integration, Pinch Technology allows for the recovery of this rejected heat and its reuse in preheating the feed or elsewhere in the process. Following the core principle of this method, heat is exchanged between hot and cold process streams at a minimum temperature approach, ensuring thermodynamic efficiency [34]. To implement this, heat exchangers are introduced to transfer both latent and sensible heat between process streams. A heat exchanger network (HEN) enables internal energy reuse by transferring heat from hot process streams (requiring cooling) to cold process streams (requiring heating). The minimum utility requirements for the external heating and cooling demands can be estimated through energy balances on the hot and cold streams as follows:

$$Q_{HS} = m_{HS} C_{P,HS}\left(T_{HS,out} - T_{HS,in}\right) \quad (16)$$

$$Q_{CS} = m_{CS} C_{P,CS}\left(T_{CS,out} - T_{CS,in}\right) \quad (17)$$

Where Q_{HS}(kW) and Q_{CS}(kW) denote the heat duties of the hot and cold streams, respectively; m_{HS}(kg·h^{-1}) is the mass flow rate of a hot stream (i.e., a stream requiring cooling), m_{CS}(kg·h^{-1}) is the mass flow rate of a cold stream (i.e., a stream requiring heating), and C_p(kJ·kg $^{-1}$·K^{-1}) represents the specific heat capacity of the stream.

In a properly integrated system, the cooling load is recovered by exchanging heat with the heating load, enabling internal circulation of process heat without the need for additional external energy input [17]. Pinch analysis facilitates the design of processes with minimum utility consumption by constructing composite heating and cooling curves on a temperature–enthalpy diagram [35]. This diagram identifies the pinch point, defined as the location of the minimum allowable temperature difference between hot and cold streams. Based on this point, the minimum thermodynamic requirements for heating and cooling can be determined, together with the overall thermal energy demand and heat-availability profiles for the entire process.

2.2.2. Energy efficiency calculation

To evaluate the energy efficiency of the process, the first and second laws of thermodynamics are applied [36]. These fundamental principles provide the basis for formulating the governing equations for column operation, including mass and energy balances and entropy generation. For each process unit, the analysis is performed under steady-state conditions, assuming steady flow and neglecting variations in kinetic and potential energies. Under these assumptions, the key equations used to assess thermodynamic efficiency are presented below, following the methodology outlined by Gutiérrez-Guerra et al. [37]:

- First law of thermodynamics:

$$\sum_{out}(nh + Q + W_s) - \sum_{in}(nh + Q + W_s) = 0 \quad (18)$$

- Second law of thermodynamics:

$$\sum_{out}\left(ns + \frac{Q}{T_s}\right) - \sum_{in}\left(ns + \frac{Q}{T_e}\right) = \Delta S_{irr} \quad (19)$$

- Exergy balance:

$$\sum_{out}\left[nb + Q\left(1 - \frac{T_0}{T_S}\right) + W_S\right] - \sum_{in}\left[nb + Q\left(1 - \frac{T_0}{T_e}\right) + W_S\right] = Lw \quad (20)$$

Where, the exergy function, b and the lost work in the system, Lw, are given, respectively by :

$$b = h - T_0 S \quad (21)$$

$$Lw = T_0 \Delta S_{irr} \quad (22)$$

Where, h, the molar enthalpy and ΔS_{irr}, the irreversible entropy

- Minimum work of separation:

$$W \sum_{out}(nb) \sum_{in}(nb)_{min} \quad (23)$$

- Second law efficiency:

$$\eta = \frac{W_{min}}{L_W + W_{min}} \quad (24)$$

The PR EOS described before can be used to calculate thermodynamic properties of the streams of the distillation column.

2.2.3. CO_2 emissions calculation

In crude oil refining, fuel is combusted to supply energy to various industrial units, including furnaces, gas turbines, and boilers. The combustion of fuel in the presence of air generates carbon dioxide (CO_2), according to the stoichiometric reaction (25).

$$C_xH_Y + \left(x + \frac{y}{4}\right) O_2 \rightarrow xCO_2 + \frac{y}{2} H_2O \quad (25)$$

Where, x and y are the carbon, C, and hydrogen, H, atoms number, respectively, present in the fuel compositions.

To estimate CO_2 emissions, the simplified model proposed by Gadalla et al. [38] is employed. In this model, excess air is assumed to ensure complete combustion. Accordingly, the CO_2 emission rate ($kg \cdot s^{-1}$) is directly proportional to the amount of fuel burned, Q_{Fuel}, in the heating device, as expressed by Eq. (26). Here, $\alpha = 3.67$denotes the ratio of the molar mass of CO_2 to that of carbon; $NHV$is the net heating value of the fuel; and $C$is the carbon content (%).

$$[CO_2]_{Emiss} = \left(\frac{Q_{Fuel}}{NHV}\right)\left(\frac{C}{100}\right)\alpha \quad (26)$$

Where, α= 3.67 is the ratio of molar masses of CO_2 and atom of carbon, C; NHV, the Net Heating Value of fuel and C, the content of Carbon (%).

In distillation columns, CO_2 emissions originate primarily from the boiler. The heat required by the process is supplied as steam generated through fuel combustion. In this context, the amount of fuel burned in the furnace can be estimated using the same expression applied in extractive distillation systems [36]. This relation links the fuel consumption rate to the process heat duty, Q_{proc}, as shown in Eq. (27), where λ_{Proc}($kJ \cdot kg^{-1}$) and h_{Proc}($kJ \cdot kg^{-1}$) are the latent heat and enthalpy of the steam delivered to the process, respectively, and T_0(°C) is the ambient temperature.

$$Q_{Fuel} = \frac{Q_{Proc}}{\lambda_{Proc}} (h_{Proc} - 419) \frac{T_{FTB} - T_0}{T_{FTB} - T_{Stack}} \quad (27)$$

The temperature difference between the flue gas inside the chimney and the surrounding environment is referred to as the stack temperature, T_{stack}, typically taken as 160 °C. The theoretical flame temperature of the furnace flue, T_{FTB}, is generally around 1800 °C [36].

3. Results and Discussion

The calculations for the LPG debutanizer and splitter columns were carried out using real industrial crude-oil data and the model equations described earlier. To perform these calculations, PRO/II software was used, as it is widely applied in refineries for simulating separation units. The software first served to check and confirm that the model was valid. Once the model was validated, it was then used to compute all the thermodynamic properties needed for this study.

3.1. Model validation

The simulations of the LPG recovery and splitter columns were conducted based on the material and energy balance equations governing the operation of the separation units, as well as the PR EOS. All these equations are detailed in Section 3. The calculated results were compared to the experimental data by determining the error, defined as follows:

$$E(\%) = \frac{|V_e - V_c|}{V_e} \times 100 \quad (31)$$

Where, V_c and V_e are the calculated and the industrial values, respectively.

Table 2 presents the simulation results of the industrial process. The model's accuracy was evaluated by comparing the predicted boiling temperatures, molar flow rates, specific gravity at 15°C (SG) of LPG and gasoline, and the mole fractions of various process streams to industrial data obtained from a functioning crude oil distillation column. These data were collected at the input and output of the two columns in the separation process. The comparison indicates that the results are satisfactory when accounting for measurement errors.

3.2. Proposed Design

By applying pinch analysis, targets were established to reduce both column size and overall energy consumption. Heat integration between the LPG recovery column and the LPG splitter was achieved through a proposed heat-exchanger network.

Figure 4 shows the configuration of the three heat exchangers used in the LPG process. In this arrangement, each exchanger functions simultaneously as the main fractionator for one column, the prefractionator for the next, and the cold stream for air-cooling duties. Energy integration focuses on linking the heating and cooling requirements within a process. During plant design, these needs are identified and addressed through a heat-exchanger network that transfers heat between hot and cold process streams, with any remaining demand supplied by utilities.

The simulation of the flow sheet shown in Figure 4 was carried out using the validated model. The operating data, such as the flow rates of the distillate and reflux streams for both columns, as well as the feed tray locations in each column, were adhered to.

Next, the pinch location and minimum heating and cooling requirements were determined using the stream data for the hot and cold streams. The transfer duties in the heat exchanger network were calculated using Eq. 16 and 17.

Table 2. Simulation results of the industrial process

Feed		Debutanizer column				Splitter column			
		Stream C5+		Stream LPG		Stream butane		Stream propane	
		V_c	E (%)	LPG	E (%)	Butane	E (%)	Propane	E (%)
T (°C)	101	142	4.05	44	4.35	95.32	8.32	66.74	13.12
P bar	11.7	9.64	7.71	8.46	0.47	18.66	9.12	17.68	5.24
N (Kmol/ h)	548.89	431.59	5.58	117.6	2.80	98.5	3.87	19.2	6.67
SG	0.623	0.68	2.86	0.55	3.77	0.566	0.88	0.52	2.36
Mol fraction									
H_2S	Trace	Trace	-	0.0014	-	trace	-	0.0035	-
H_2	Trace	Trace	-	trace	-	trace	-	trace	-
C1	Trace	Trace	-	trace	-	trace	-	trace	-
C2	0.0006	Trace	-	trace	-	trace	-	trace	-
C3	0.0896	Trace	-	0.2253	9.88	0.0120	9.18	0.9687	1.15
iC4	0.1092	0.0070	-	0.3905	4.99	0.4571	8.83	0.0052	6.75
C4	0.1210	0.0030	9.61	0.3759	1.61	0.5267	7.60	0.0007	-
iC5	0.2157	0.4020	0.69	0.0094	4.58	0.0008	0.09	trace	-
C5	0.1629	0.1820	4.12	0.0007	5.58	0.0006	-	trace	-
C6+	0.3032	0.4160	1.46	trace	-	trace	-	trace	-

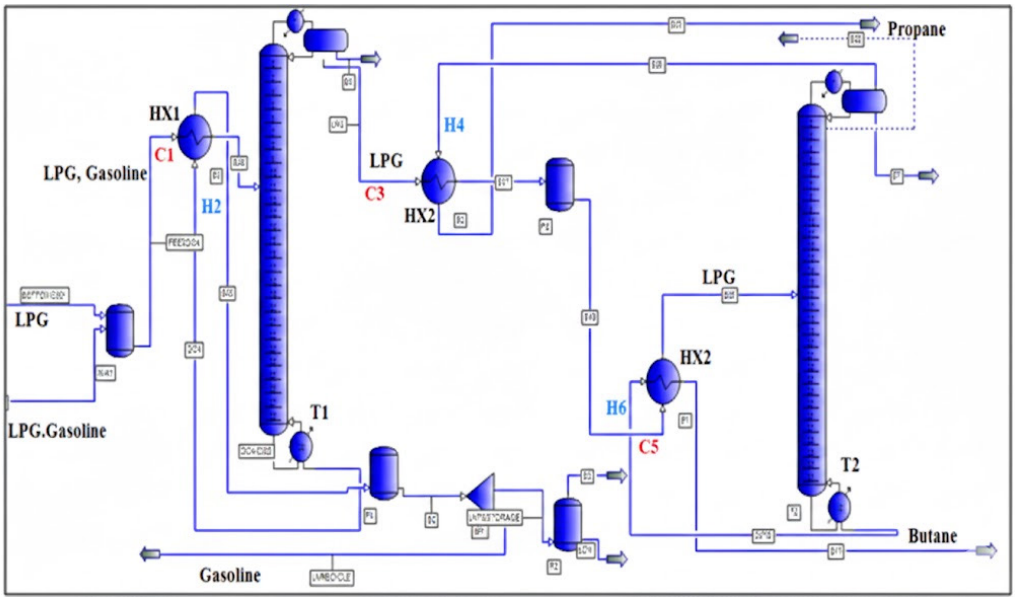

Fig. 4. Simplified schematic of the LPG Integration process (C_i, cooled stream; H_i; heat stream)

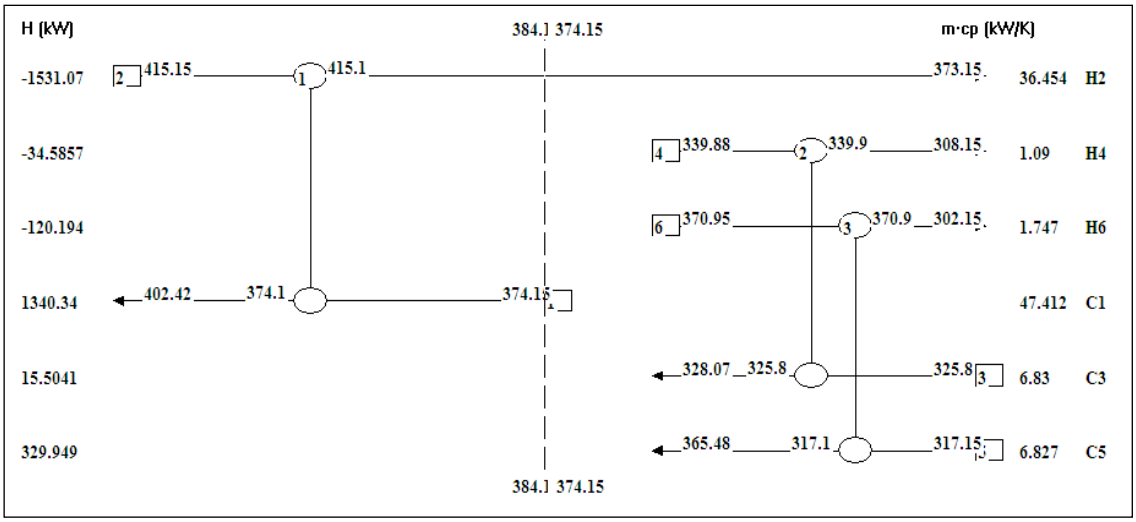

Fig. 5. Temperature intervale analyses in heat exchanger network

Calculate ΔTmin:

The minimum temperature difference is the direct difference between the hot and cold pinch temperatures:

- Hot pinch temperature: $T_{H,\text{Pinch}} = 384.1\ \text{K}$
- Cold pinch temperature: $T_{C,\text{Pinch}} = 374.15\ \text{K}$

So the minimum approach temperature is:

$$\Delta T_{\min} = T_{H,\text{Pinch}} - T_{C,\text{Pinch}}$$

$$\Delta T_{\min} = 384.1\ \text{K} - 374.15\ \text{K} = 9.95\ \text{K}$$

$$\boxed{\Delta T_{\min} = 9.95\ \text{K}}$$

The Grand Composite Curve (GCC) reveals that the process achieves an exceptionally high degree of thermal integration, with both the minimum hot utility and minimum cold utility effectively reduced to zero, indicating that all heating and cooling demands are satisfied through internal heat exchange. The Pinch Point, located at 370.9 K where the cumulative enthalpy reaches its minimum value of –1685.85 kW, delineates the boundary between the heat-demanding region above the pinch and the heat-releasing region below it. In accordance with pinch principles, no heat transfer occurs across this temperature level, ensuring that all heating requirements above the pinch are supplied by internal hot streams, while all excess heat below the pinch is absorbed by internal cold streams (Figure 6).

The maximum internal heat recovery, quantified as 1685.85 kW, represents the full thermodynamic potential for energy savings within the system. Overall, the GCC confirms that the proposed heat exchanger network operates near theoretical optimality, maximizing energy efficiency and minimizing reliance on external utilities.

3.3. Performance of LPG process

The performance of the optimized process was analyzed based on the calculation of energy efficiency and the concentration of carbon dioxide emissions. Energy efficiency was calculated following the procedure outlined in Section 4.2, while the CO2 concentration was derived from equations 26 and 27.

The necessary thermodynamic properties, such as enthalpies, entropies of streams, and heat duties, were determined through simulation.

The main results obtained were compared to those of the conventional process. This comparison is presented in Table 3.

The table shows that, compared to the conventional process, the new configuration for the LPG separation process increases energy efficiency and reduces the concentration of carbon dioxide emissions. With the new heat exchanger network design, energy consumption is lower than in the previous case. The new process requires 6200 kW to complete the separation, with an energy efficiency of 86%.

In contrast, the conventional process requires 8100 kW of heat duties to achieve the separation, with an overall energy efficiency of 74%. Notably, the heat duty of the air-cooled system, Q_{AC}, is 500 kW in the conventional process. Figure 7 illustrates the comparison between the industrial and optimized processes for LPG separation in a crude oil refinery.

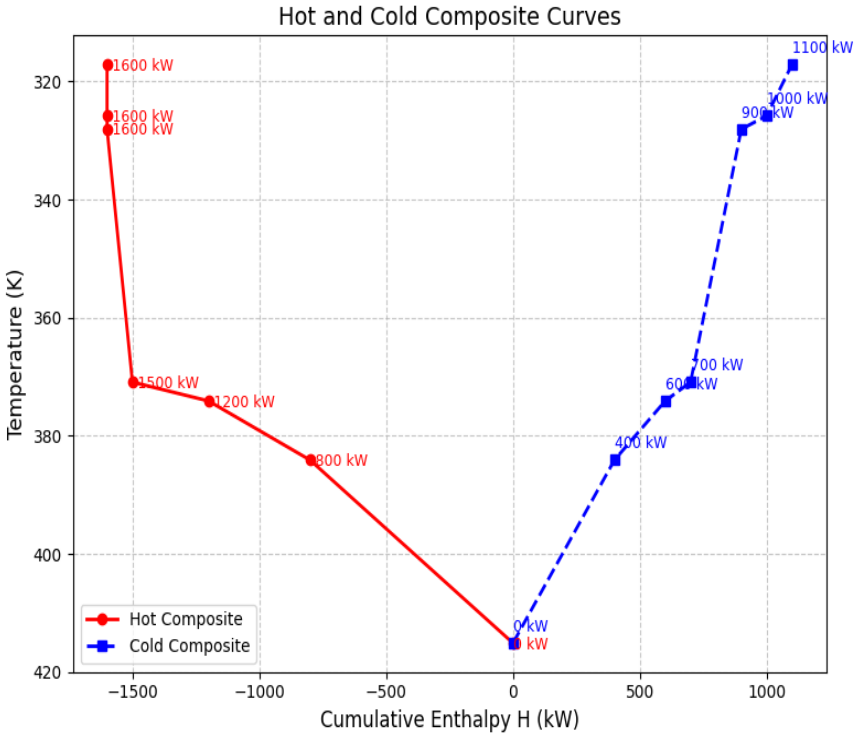

Fig. 6. GCC Curves

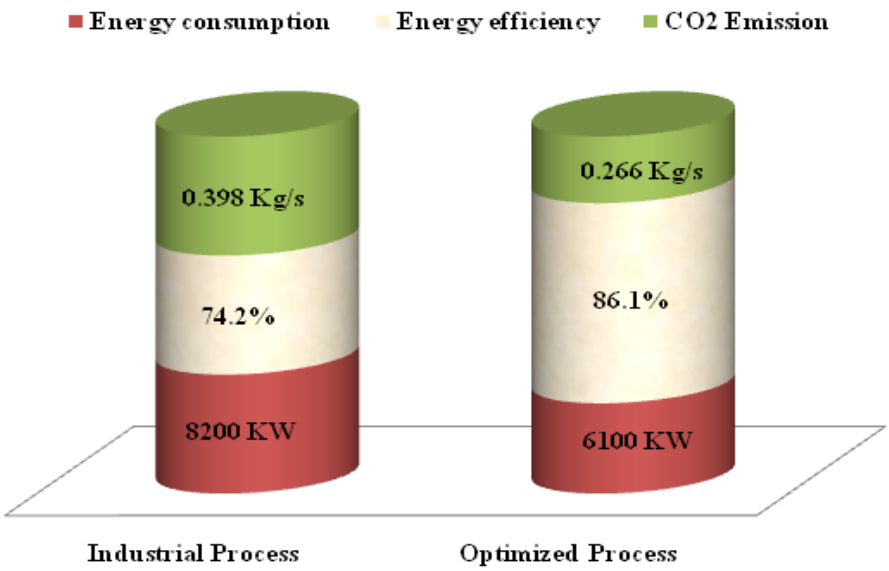

Fig. 7. Performance comparison between industrial and optimized process

Table 3. Performance of LPG process before and after integration of Heat exchanger

Stream	Conventional process		Optimized process	
	Debutanizer colum	Splitter column	Debutanizer colum	Splitter column
Q_{AC} (kW)	-	500	-	-
Q_c (kW)	-2900	-200	-3000	-200
Q_r (kW)	4000	500	2700	300
W_{min} (kW)	2650	450	2180.4	260
L_W (kW)	1380	90	495.7	25
Ƞ	0.65	0.83	0.81	0.91
$[CO_2]_{Emission}$ (Kg/s)	0.354	0.044	0.239	0.027

4. Conclusion

In this study, the primary objective was to enhance the energy efficiency of the LPG debutanizer and splitter columns in an operating industrial oil refinery. The governing model equations for the separation process were first validated through simulations using industrial plant data, and the resulting predictions exhibited an acceptable deviation from measured values, confirming the model's suitability for the refinery under investigation. Subsequently, a new LPG separation configuration was developed and evaluated using pinch analysis. The thermodynamic properties required for this assessment were generated with Pro/II software employing the Peng–Robinson (PR) equation of state, enabling an accurate characterization of the thermal behavior of the process streams.

The results demonstrated that integrating three heat exchangers into the conventional configuration significantly reduced energy consumption, improved overall thermal efficiency, and lowered CO_2 emissions. Specifically, the application of energy integration techniques achieved a 23.46% reduction in energy consumption and a 33.17% decrease in CO_2 emissions relative to the existing industrial process. These findings underscore the effectiveness of thermal integration strategies in enhancing process sustainability and reducing the environmental footprint of refinery operations.

Nomenclature

a: energy parameter of the EOS (J m^3/kmol)
b: volume parameter of the EOS (m^3/kmol)
H: Enthalpy of vapor (kJ/kg)
h: Enthalpy of liquid (kJ/kg)
L: liquid flow rate (kg/h)
R: ideal gas constant = 8314.5 J/kmol/K
U: Liquid side stream, (kg/h)
V : Vapor flow rate, (kg/h)
v: Volume (m^3)
W: Vapor sidestream (kg/h)
x_i: liquid phase mole fraction of component i
y_i : vapor phase mole fraction of component i
z_i : mole fraction of component i
Z: compressibility factor
f_i^L: Fugacity of component i in liquid phase
f_i^V: Fugacity of component i in vapor phase
k_{ij} binary interaction parameter between component i and j.
N: Feed flow rate (kg mol/h)
P: pressure (bar)
SG: Specific gravity
T: temperature (K)
Q: heat flow (kw h)
Cp: heat capacity
m_{HS}: the flow rate of haut stream
m_{CS}: the flow rate of could stream

s: Entropy
h: Enthalpy
b: Exergy
W: travail
E: Energy
Ŋ: Energy efficiency

Abbreviations
EOS: equation of state
LPG: Liquefied Petroleum Gas
PR : Peng-Robinson
VLE: vapor liquid equilibria
H_i: Heat streams
C_i : Cold streams
HX: Heat exchanger

Greek letters
ω: acentric factor
ϕ_i^L: Fugacity coefficient of component i in liquid phase
ϕ_i^V: Fugacity coefficient of component i in Vapor phase

References

[1] S. Faramawy, T. Zaki and A. Sakr, Natural gas origin, composition, and processing: A review. *J. Nat. Gas Sci. Eng.*, 34 (2016) 34-54.

[2] I. Malinen and J. Tanskanen, Thermally Coupled Side-Column Configurations Enabling Distillation Boundary Crossing. 2. An Overview and a Solving Procedure. *Ind. Eng. Chem. Res.*, 48 (2009) 6387–6404.

[3] L. T. Biegler, I. E. Grossmann and A. W. Westerberg, Systematic methods of chemical process design, Prentice Hall Inc, New Jersey (1997).

[4] I. Karimi and R. Srinivasan, 11th International Symposium on Process Systems Engineering 1st Ed., National University of Singapore, Singapore (2012).

[5] A. Bahadori, Natural Gas Processing 1st Ed., Gulf Professional Publishing (2014) 547–590.

[6] K. Matsuda, K. Kawazuishi, Y. Kansha, C. Fushimi, M. Nagao, H. Kunikiyo et al., Advanced energy saving in distillation process with self-heat recuperation technology. *Energy*, 36 (2011) 4640-4645.

[7] B. Suphanit, Optimal heat distribution in the internally heat-integrated distillation column (HIDiC). *Energy*, 36 (2011) 4171-4181.

[8] A. Kiss, J. Servando, L. Flores, A. Carlos and I. Ferreira, Towards energy efficient distillation technologies – Making the right choice. *Energy*, 47 (2012) 531-542.

[9] M. A. Waheed, A. O. Oni, S. B. Adejuyigbe and B. A. Adewumi, Thermoeconomic and environmental assessment of a crude oil preheat train using artificial neural networks. *Appl. Therm. Eng.*, 66 (2014) 191-205.

[10] A. Ould Brahim, S. Abderafi and T. Bounahmidi, Parametric study on the energy efficiency of the stabilization column. *IEEE*, (2016) 1-5.

[11] A. Tgarguifa, S. Abderafi and T. Bounahmidi, Energetic optimization of Moroccan distillery using simulation and response surface methodology. *Renew. Sustain. Energy Rev.*, 75 (2017) 415-425.

[12] C. Li, X. Zhanga, S. Zhang and K. Suzuki, Environmentally conscious design of chemical processes and products: Multi-optimization method. *Chem. Eng. Res. Des.*, 87 (2009) 233–243.

[13] M. Gadalla, Ž. Olujić, M. Jobson and R. Smith, Estimation and reduction of CO2 emissions from crude oil distillation units. *Energy*, 31 (2006) 2398–2408.

[14] A. Szklo and R. Schaeffer, Fuel specification, energy consumption and CO2 emission in oil refineries. *Energy*, 32 (2007) 1075–1092.

[15] F. N. Osuolale and J. Zhang, Energy efficiency optimisation for distillation column using artificial neural network models. *Energy*, 106 (2016) 562-578.

[16] M. A. Al-Mayyahi, A. F. A. Hoadley and G. P. Rangaiah, Energy optimization of crude oil distillation using different designs of pre-flash drums. *Appl. Therm. Eng.*, 73 (2014) 1204-1210.

[17] M. A. Waheed and A. O. Oni, Performance improvement of a crude oil distillation unit. *Appl. Therm. Eng.*, 75 (2015) 315-324.

[18] S. V. Inamdar, S. K. Gupta and D. N. Saraf, Multi-objective Optimization of an Industrial Crude Distillation Unit Using the Elitist Non-Dominated Sorting Genetic Algorithm. *Chem. Eng. Res. Des.*, 82 (2004) 611–623.

[19] M. L. Ochoa-Estopier, M. Jobson and R. Smith, The use of reduced models for design and optimisation of heat-integrated crude oil distillation systems. *Energy*, 75 (2014) 5-13.

[20] M. A. Samborskayaa, V. P. Guseva, I. A. Gryaznova, N. S. Vdovushkina and A. V. Volf, Crude Oil Distillation with Superheated Water Steam: Parametrical Sensitivity and Optimization. *Procedia Chem.*, 10 (2014) 337–342.

[21] A. Nemati Rouzbahani, M. Bahmani, J. Shariati, T. Tohidian and M. R. Rahimpour, Simulation, optimization, and sensitivity analysis of a natural gas dehydration unit. *J. Nat. Gas Sci. Eng.*, 21 (2014) 159-169.

[22] H. Wang, X. Cui, R. Wang and C. Li, Response surface optimization of the operating parameters for a complex distillation column based on process simulation. *Energy Procedia*, 16 (2012) 571–578.

[23] E. Díez, P. Langston, G. Ovejero and M. D. Romero, Economic feasibility of heat pumps in distillation to reduce energy use. *Appl. Therm. Eng.*, 29 (2009) 1216–1223.

[24] M. Errico, G. Tola and M. Mascia, Energy saving in a crude distillation unit by a preflash implementation. *Appl. Therm. Eng.*, 29 (2009) 1642–1647.

[25] X. G. Liu, C. He, C. C. He, J. J. Chen, B. J. Zhang and Q. L. Chen, A new retrofit approach to the absorption-stabilization process for improving energy efficiency in refineries. *Energy*, 118 (2017) 1131-1145.

[26] B. Hussain and M. Ahsan, A Numerical Comparison of Soave Redlich Kwong and Peng-Robinson Equations of State for Predicting Hydrocarbons' Thermodynamic Properties. *Eng. Technol. Appl. Sci. Res.*, 8 (2018) 2224-2226.

[27] K. Matsuda, K. Kawazuishi, Y. Kansha, C. Fushimi, M. Nagao, H. Kunikiyo et al., Advanced energy saving in distillation process with self-heat recuperation technology. *Energy*, 36 (2011) 4640-4645.

[28] L. T. Biegler, Nonlinear Programming Concepts Algorithms and Applications to Chemical Processes, Carnegie Mellon University, Pennsylvania (2010).

[29] G. M. Kontogeorgis and G. K. Folas, Thermodynamic Models for Industrial Applications: From Classical and Advanced Mixing Rules to Association Theories, John Wiley & Sons Ltd (2010).

[30] D. Y. Peng and D. B. Robinson, A New Two-Constant Equation of State. *Ind. Eng. Chem. Fundam.*, 15 (1976) 59–64.

[31] J. M. Prausnitz, R. N. Lichtenthaler and E. G. Azevedo, Molecular Thermodynamics of Fluid Phase Equilibria; 3rd ed., Prentice-Hall, New Jersey (1999).

[32] I. C. Kemp, Pinch Analysis and Process Integration: A user Guide on Process Integration for the Efficient Use of Energy, Butterworth-Heinemann (2006).

[33] R. Smith, Chemical Process Design, McGraw-Hill, New York (1995).

[34] B. Linnhoff and J. R. Flower, Synthesis of heat exchanger networks: I. Systematic generation of energy optimal networks. *AIChE J.*, 24 (1978) 633–642.

[35] B. Linnhoff and E. Hindmarsh, The pinch design method for heat exchanger networks. *Chem. Eng. Sci.*, 38 (1983) 745-763.

[36] H. Al-Muslim and I. Dincer, Thermodynamic analysis of crude oil distillation systems. *Int. J. Energy Res.*, 29 (2005) 637-655.

[37] R. Gutiérrez-Guerra, J. G. Segovia-Hernández and S. Hernandez, Reducing energy consumption and CO2 emissions in extractive distillation. *Chem. Eng. Res. Des.*, 87 (2009) 145–152.

[38] A. M. Gadalla, Z. Olujic, P. J. Jansens, M. Jobson and R. Smith, Reducing CO2 emissions and energy consumption of heat-integrated distillation systems. *Environ. Sci. Technol.*, 39 (2005) 6860-6870.

[39] A. M. Eliceche, M. C. Daviou, P. M. Hoch and I. O. Uribe, Optimisation of azeotropic distillation columns combined with pervaporation membranes. *Comput. Chem. Eng.*, 26 (2002) 563–573.

[40] M. R. Hojjati, M. R. Omidkhah and M. H. Panjeh Shahi, Cost Effective Heat Exchanger Network Design with Mixed Materials of Construction. *Iran. J. Chem. Chem. Eng.*, 23 (2004) 89-100.